

# Landslide susceptibility mapping along Kolli hills Ghat road section (India) using frequency ratio, relative effect and fuzzy logic models

V. Ramesh · S. Anbazhagan

Received: 26 January 2014 / Accepted: 10 December 2014 / Published online: 23 December 2014  
© Springer-Verlag Berlin Heidelberg 2014

**Abstract** This article emphasizes landslide susceptibility mapping along Ghat road of Kolli hills, Tamil Nadu, India, using frequency ratio, relative effect and fuzzy gamma operator models with the help of remote sensing data and GIS technique. The purpose of the study is to generate, compare and validate landslide susceptibility zones. Landslide inventory was done with data collected from the State Highways department. There are nine landslide-influencing parameters such as slope gradient, slope aspect, slope curvature, relief, lithology, land use and land cover, proximity to road, proximity to drainage, and proximity to lineament, analyzed with help of topo map, existing geology map and satellite data to produce landslide susceptibility maps. Landslide susceptibility maps were generated by calculating relationship between the landslide-influencing factors with past landslide locations using frequency ratio, relative effect and fuzzy gamma operator models. These landslide susceptibility maps were verified and compared using the existing landslide inventory data. The prediction accuracy of frequency ratio model was 87.93 %, for fuzzy gamma operator model was 87.33 %, and for relative effect model it was 85.26 %. Out of which, the frequency ratio model provide maximum prediction accuracy on landslide susceptibility.

**Keywords** Landslide susceptibility · Frequency ratio model · Relative effect model · Fuzzy gamma operator · Kolli hills

## Introduction

Landslide is one of the important natural calamities, which commonly occurred on cut slopes of Ghat roads in mountainous region, while events are also reported in residential areas causing risk to human life, property loss, damage to established road network, and buildings in each year (Aleotti and Chowdhury 1999; Lee and Pradhan 2007; Nandi and Shakoor 2008). Landslides also occur in natural slopes, influenced by various geo-environmental parameters and triggered by rainfall and earthquakes. The natural slopes converted into cut slopes by human intervention for the purpose of transportation network, construction of dams, bridges, and tunnels are more prone to landslide occurrences (Das et al. 2010; Singh et al. 2013a, b). In mountainous terrain, landslides are natural denudation process and its occurrence is subjected to various causative factors and triggered by several external factors such as seismicity, rainfall, water level change, storm waves, and rapid stream erosion (Naranjo et al. 1994; Dai et al. 2002). Hill slopes in mountainous areas are affected by human activities such as building road network, urban development, deforestation, and rapid land use modification, may also influence occurrence of landslides (Das et al. 2011).

The demarcation and mitigation of landslide-prone areas in a region is crucial for future planning and developmental activities. Many Government organizations and several research institutions have spent significant funds to evaluate the landslide hazards and their spatial distribution (Guzzetti et al. 1999). The landslide hazard and susceptibility mapping is an important task for geoscientists, planners and local administrations, as knowledge about the socioeconomic worth of landslides has increased globally (Devoli et al. 2007). Landslide susceptibility refers to the probability of landslide occurrence in a region based on the

---

V. Ramesh · S. Anbazhagan (✉)  
Centre for Geoinformatics and Planetary Studies,  
Department of Geology, Periyar University, Salem, India  
e-mail: anbu02@gmail.com

relationship between causative factors with spatial distribution of landslides (Brabb 1984). Landslide susceptibility mapping describes the type, spatial extent and intensity of past and present landslides in the study area to assess the probable areas for future landsliding, but the frequency or timing is not incorporated (AGS 2007; Anderson and Holcombe 2013). Landslide hazard zonation mapping provides the details about the possible landslide occurrence of a certain type and magnitude in a particular location within a set time (Varnes 1984). Landslide susceptibility maps show the zones, which are stable and possible zones for future landslide occurrence (Corominas and Moya 2008).

The methods of landslide hazard and susceptibility assessment techniques by Mantovani et al. (1996) includes distribution analysis (Wieczorek 1984), qualitative analysis (Kienholz et al. 1984; McKean et al. 1991), statistical analysis (Yin and Yan 1988; Gupta and Joshi 1990; Carrara et al. 1991; Wang and Unwin 1992; Pachauri and Pant 1992; Sarkar et al. 1995; Mark and Ellen 1995; Chung and Fabbri 1999; Lee et al. 2002; Ayalew et al. 2004), deterministic analysis (Skempton and Delory 1957; Okimura 1982; Okimura and Kawatani 1986; Mostyn and Fell 1997; Singh et al. 2013a, b; Ahmad et al. 2013), landslide frequency analysis (Capecechi and Focardi 1988), and distribution-free methods such as fuzzy and ANN. Several studies have been carried out for estimating the spatial probability of landslide occurrences using GIS technique. Many landslide studies were conducted using probabilistic models such as frequency ratio and logistic regression (Atkinson and Massari 1998; Dai et al. 2001; Dai and Lee 2002; Ohlmacher and Davis 2003; Lee et al. 2004; Wang and Sassa 2005; Lee 2005; Lee and Talib 2005; Lee and Pradhan 2006, 2007; Akgul and Bulut 2007; Akgun et al. 2008; Pradhan et al. 2008; Tunusluoglu et al. 2008; Yilmaz 2009a; Yilmaz and Keskin 2009; Ehret et al. 2010; Kannan et al. 2013) and some studies adopted using relative effect model (Ghafoori et al. 2006; Naveen Raj et al. 2011). As a new approach to assess landslide hazards such as fuzzy logic (Ercanoglu and Gokceoglu 2001; Lee 2007; Champati Ray et al. 2007; Kavitha et al. 2008; Kanungo et al. 2009; Pradhan et al. 2009; Srivastava et al. 2010) artificial neural network models were adopted (Lee et al. 2003, 2006; Caniani et al. 2008; Pradhan and Lee 2007, 2010a; Yilmaz 2009b; Poudyal et al. 2010; Chauhan et al. 2010; Choi et al. 2012). In the present study, landslide susceptibility mapping along Ghat road section of Kolli hills was carried out using frequency ratio (FR), fuzzy gamma operator and relative effect (RE) models. The resultant susceptibility maps were compared and prediction accuracies of each map were derived for further evaluation.

## Study area

Kolli hills is one of the important tourist spots in Tamil Nadu situated in the tail end of the Eastern Ghats in Namakkal district of Tamil Nadu, India (Fig. 1). The hills cover an area of 283 km<sup>2</sup> with an elevation ranges between 1,000 and 1,390 m above mean sea level (MSL). It has mild climate and the location is known for herbal cultivation. Recently, the region of Kolli hills became taluk (administrative boundary) and the total population is 63,888 according to 2001 census covered in 14 villages. The geological assessment in the study area has shown that charnockitic group of rocks, widely present in the north-eastern part of Tamil Nadu State, are well exposed in many prominent hill ranges such as Pallavaram–Chengleput, Javadi, Shevaroy, Chitteri, Kalrayan, Kollimalai (Kolli hills), Pachchaimalai and Nilgiri. In the central part of the State, Kolli hills is situated as a residual plateau-topped charnockitic hill surrounded by pediments and pediplains. Laterite associated with reddish brown ferruginous clayey soil caps on the crystalline rocks at high altitude of Kolli hills derived by the sub-aerial weathering of charnockites and exposed as patches. Irregular lenses and pockets of bauxite and lateritic bauxite are occurring over charnockites at 1,148–1,386 m altitudes above mean sea level (GSI 2006).

The Ghat road with 20 km stretch along 70 hairpin bends connects the foot hills at Karavallikkombai to hill top at Sholaikkadu and is chosen for the present work as study area. The Ghat road falls in between 11°18'29.72"N and 11°19'50.38"N latitudes and 78°19'30.99"E and 78°21'6.49"E longitudes. At present, this Ghat road is the main route to reach the Kolli hills and it aligned in the western slope of Kolli hills. The Ghat road was constructed along cut slopes by modifying the original natural slope condition. Hence, most of the hairpin bends are associated with vertical slope cut rock and soil profiles. These profiles are being exposed to weathering and soil erosion continuously. The major rock types along this Ghat road are charnockites and gneisses, which are mostly fractured and highly weathered. Anbazhagan et al. (2008) have studied the developments of fractures and land subsidence in the south-eastern fringe of Kolli hills due to change of natural slope and drainage condition for cultivation practices indicating frequent slope failure. The structural (discontinuities) and geological (lithology and weathering condition) parameters are the main causative factors, which influence the occurrence of landslides. The topographical factors such as slope gradient, slope aspect, slope curvature and relief are equally important in landslide occurrences. The anthropogenic activities such as deforestation, widening of roads are the common causative factors. Finally, rainfall is the major triggering factor in occurrence of

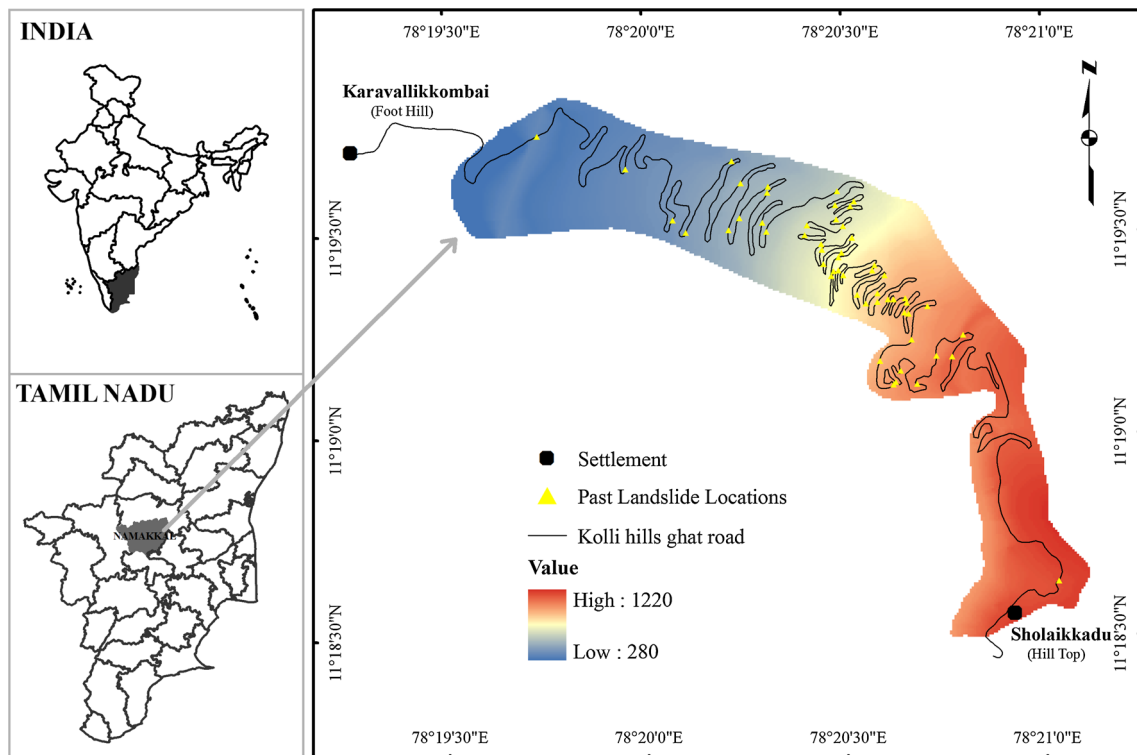


**Fig. 1** Location and digital elevation model (DEM) of Kolli hills Ghat road section along with distribution of past landslide locations

landslides in Kolli hills (Anbazhagan and Ramesh 2014). Landslips, rock fall and debris slides are the common type of mass movements observed in the Ghat road section.

**Geospatial database**

Identification of suitable landslide causative factors and its mapping need prior knowledge about the major causes of landslides (Guzzetti et al. 1999). Landslide susceptibility mapping needs data collection and construction of a geospatial database to derive landslide-influencing factors. Slope gradient, slope aspect, slope curvature, relief, lithology, land use and land cover, proximity to road, proximity to lineament, and proximity to drainage are the major landslide-influencing factors considered for the landslide susceptibility mapping along Ghat road of Kolli hills.

**Landslide inventory**

The inventory about the past landslide locations consists of the information about the existing landslides in an area, which is helpful to validate the landslide susceptibility map. An understanding of conditions and processes which influences past landslide occurrences and their evidences is the most significant aspect in the prediction of future

landslides (Yilmaz et al. 2012). In the present study, landslide inventory mapping has been carried out by collection of existing historical reports and photographs from highways department, newspaper records, and enquiry made from local people. Through data collection, it was inferred that about 74 major and minor landslide events with different intensity occurred at 54 locations. These 54 past landslide locations were collected and plotted as point feature along Ghat road section digitized from high-resolution satellite image. In the present case, it is difficult to represent the landslide areal extent in the form of polygon feature, because the landslide areas are too small to highlight in the current scale (Yilmaz 2009a). Hence, the inventory locations are entered as point feature. The inventory map depicts that occurrence of landslides was distributed all along the Ghat road (Fig. 1). Debris slide and rock fall are the most common types of landslides along the Ghat road (Fig. 2).

**Factors derived from digital elevation model**

Surface topography decides the flow sources and controls the run-off direction, which limits the density and spatial extent of landslides (Sujatha et al. 2012). A digital elevation model (DEM) with 10 m resolution was generated from 20 m interval contours digitized from 1:50,000 scale topographic map. From DEM, the slope gradient, slope

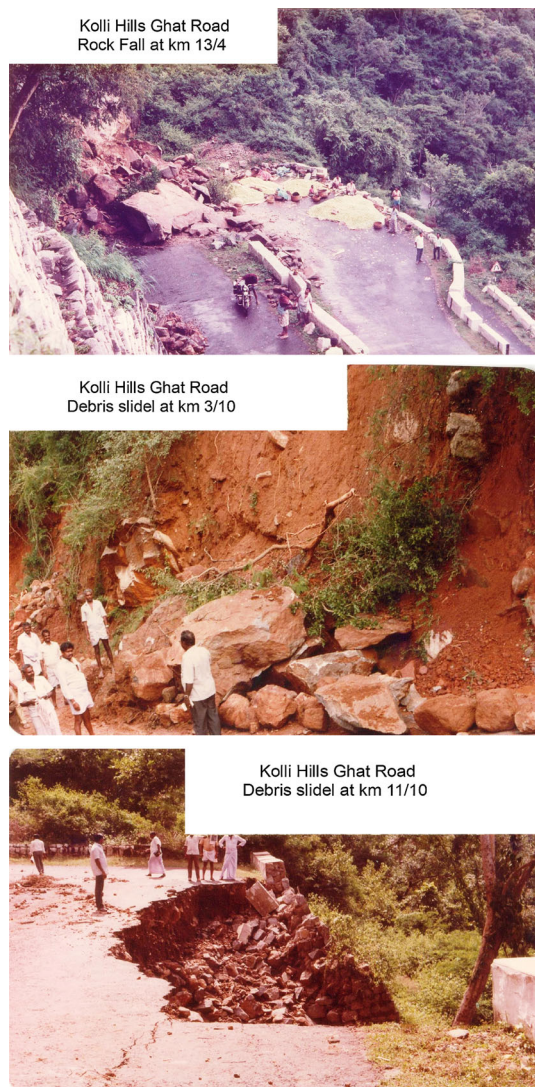


**Fig. 2** Field photographs show past landslide occurrences

aspect, slope curvature and relief were derived using the Spatial Analyst tool of ArcMap 9.1 © ESRI.

### *Slope gradient*

Slope gradient is an important factor in assessment of slope stability, which measures the rate of change of elevation in the direction of steepest fall and gravity supports the flow of water and other material in the direction of slope. It is having great importance in hydrology and geomorphology, which disturbs the speed of surface and subsurface flows (Anbalagan 1992; Ercanoglu and Gokceoglu 2004; Kannan et al. 2013). The slope gradient map (Fig. 3a) was reclassified into five classes viz.,  $<13^\circ$ ,  $13\text{--}22^\circ$ ,  $22\text{--}32^\circ$ ,  $32\text{--}45^\circ$ , and  $>45^\circ$ , following the Jenks natural breaks classification method (Jenks 1967).

**Fig. 3** Landslide causative factors; **a** slope gradient, **b** slope aspect, **c** slope curvature, **d** relief, **e** lithology, **f** land use and land cover, **g** road buffer, **h** proximity to drainage, **i** proximity to lineament

### *Slope aspect*

Slope aspect describes the direction of slope. Aspect shows a strong inheritance from bedrock structure and influences the exposition to sun and thereby changes in vegetation and evapotranspiration (Fernandez Merodo et al. 2004). The slope aspect (Fig. 3b) is divided into eight directional classes as N ( $337.5^\circ\text{--}22.5^\circ$ ), NE ( $22.5^\circ\text{--}67.5^\circ$ ), E ( $67.5^\circ\text{--}112.5^\circ$ ), SE ( $67.5^\circ\text{--}157.5^\circ$ ), S ( $157.5^\circ\text{--}202.5^\circ$ ), SW ( $202.5^\circ\text{--}247.5^\circ$ ), W ( $247.5^\circ\text{--}292.5^\circ$ ), and NW ( $292.5^\circ\text{--}337.5^\circ$ ). Apart from that few pixels are fall in Flat ( $-1$ ) region. Slope aspect in eight directional classes is generally adopted by many workers (Sarkar and Kanungo 2004; Kanungo et al. 2006; Pradhan and Lee 2010a). In the present study, most of the landslide locations fall in NW and W slope directions.

### *Slope curvature*

In general, curvature is defined as the curvature of a line formed by intersection of a random plane with the surface (Duman et al. 2006; Ramani et al. 2011). In the present study, the combo curvature which is the combination of plane and profile curvature is taken into consideration. The characterization of slope morphology and flow can be analyzed with the help of combo curvature map (Catani et al. 2013). In the case of curvature map, the negative values were classified as concave, the positive values were classified as convex, and zero values classified as flat (Fig. 3c). The major part of Ghat road section is covered by convex slope, followed by concave and flat condition. The maximum numbers of (24) past landslides were located in convex slope, and then 18 landslide locations were fall in flat slope.

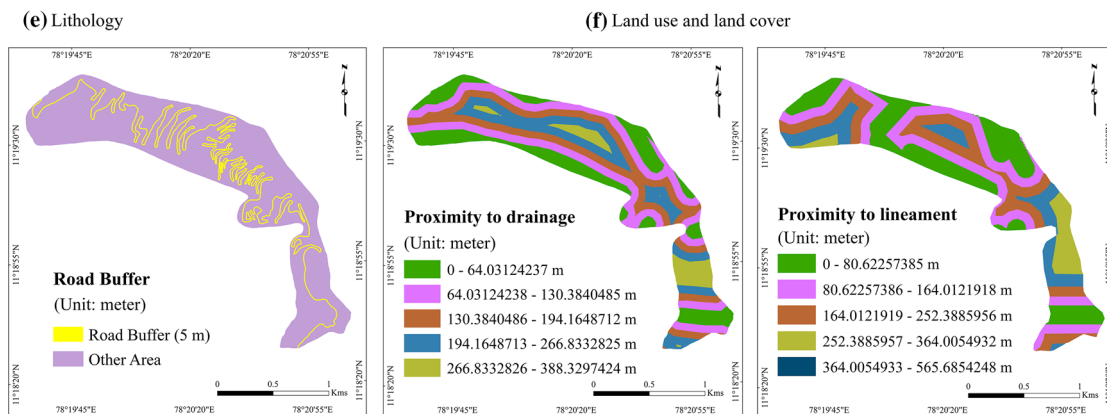
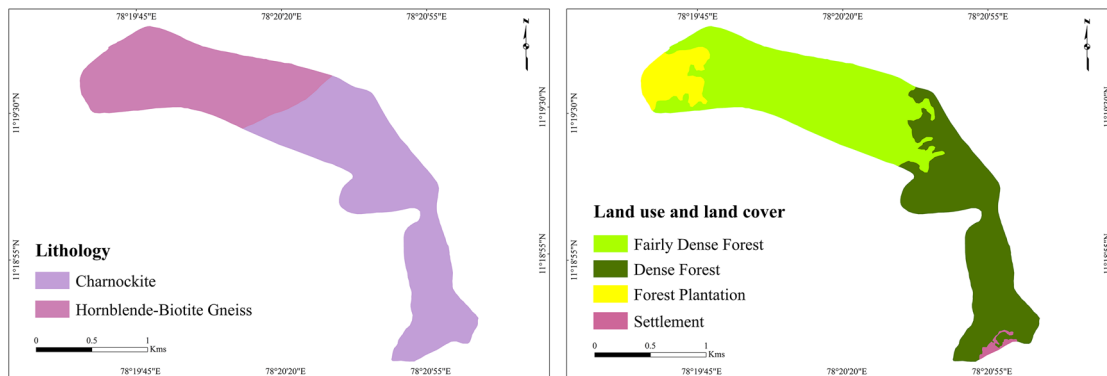
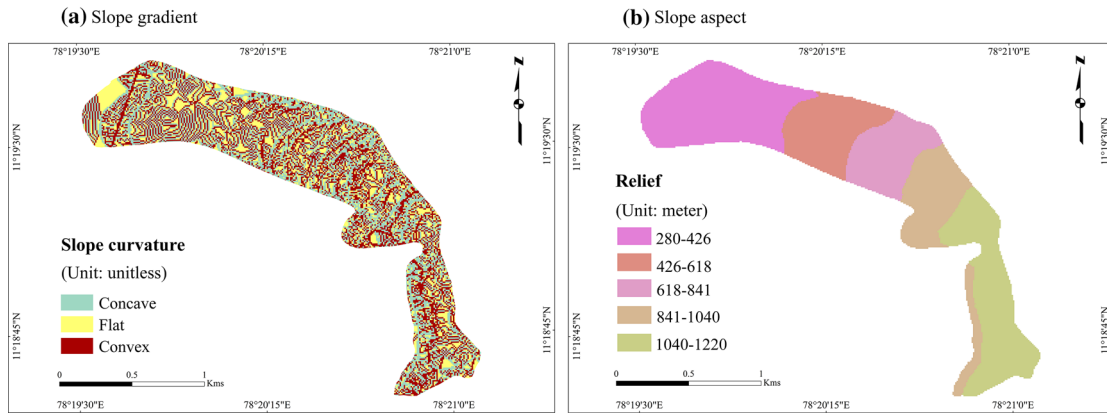
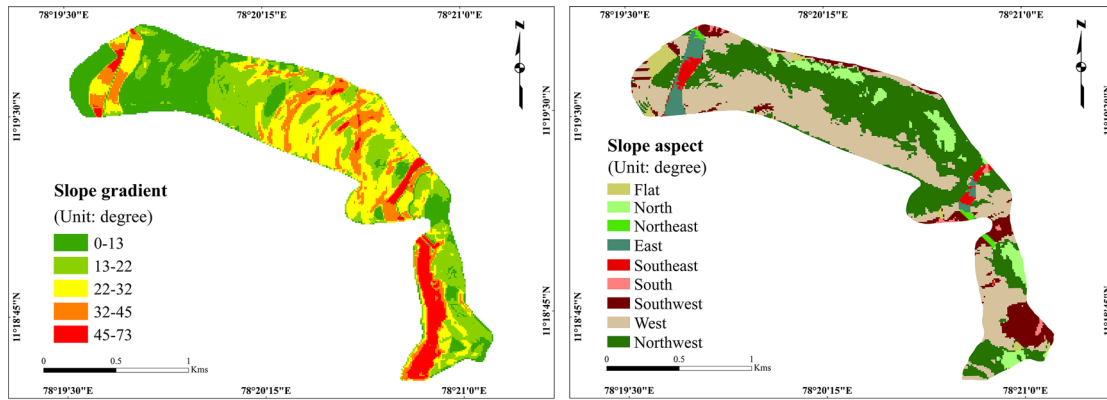
### *Relief*

Elevation is useful to understand the local relief and determines the maximum and minimum heights within the study area. In the present study area, the relief varies from 280 to 1,220 m. On the basis of Jenks natural breaks classification (Jenks 1967), the relief range was classified into five classes viz., 280–426, 426–618, 618–841, 841–1,040, and 1,040–1,220 m (Fig. 3d).

### *Geological parameters*

The lithology map of the study area is prepared from a 1:50,000 scale geological map published by GSI (1995).





(g) Proximity to road

(h) Proximity to drainage

(i) Proximity to lineament

The charnockite and hornblende–biotite gneiss are the major lithological units shown in Fig. 3e. The land use and land cover were interpreted from IRS-P6 LISS IV satellite image with 5.8 m spatial resolution acquired in the year 2006. The remotely interpreted details were verified in the field. The presence of vegetation increases erosion resistance while barren slopes are susceptible to landslides (Dai and Lee 2002). Fairly dense forest, dense forest, forest plantation, and settlement are the various land use and land cover units recognized (Fig. 3f). Most of the road section is covered by structural hill system.

### Proximity analysis

Modification of natural slope as cut slope in road construction is the most significant anthropogenic activity which causes slope instability. Road sector acts as a barrier or a path for water flow, depending on its location in the basin, may trigger occurrence of landslide (Pradhan and Lee 2010b). Since, most of the landslides were located at short distance from the road, a 5 m buffer zone was generated and considered in the present study (Fig. 3g).

The drainage map of the study area was prepared with the help of Survey of India topographical map on 1:50,000 scale. The influence of drainage on occurrence of landslide may vary in space depending upon the distance of the source area from the original stream flow (Srivastava et al. 2010). Numerous local planes of weakness were interpreted from high-resolution satellite imagery as lineaments. The occurrences of landslides are expected more in zones that fall close to these planes and less away from them. The distance from drainage and lineament was calculated using euclidean distance method in ArcGIS 9.1, and reclassified into five classes (Fig. 3h, i), based on Jenks natural breaks classification (Jenks 1967).

## Methods

### Frequency ratio (FR) model

Frequency ratio approach is based on the observed relationships between landslide distribution and each landslide-influencing factor. The relationship provides the correlation between landslide occurrence location and the factors influencing landslide in the study area. The frequency ratio of each class in a thematic layer was calculated from their relationship with past landslide events. In the relationship analysis, the ratio is that of the area where landslides occurred to the total area, so that a value of 1 is an average value. If the value is greater than 1, it means a higher correlation, and a value lower than 1 means lower correlation. The frequency ratios of each thematic layer

were then summed to estimate the landslide susceptibility index (LSI) (Eq. 4) (Lee and Talib 2005; Lee and Pradhan 2007).

$$\text{Frequency ratio} = \frac{\text{Slide ratio}}{\text{Class ratio}} \quad (1)$$

where,

$$\text{Slide ratio} = \frac{\text{Number of landslide grids in class}}{\text{Total number of landslide grids}} \quad (2)$$

$$\text{Class ratio} = \frac{\text{Number of grids in individual class}}{\text{Total number of grids in whole class}} \quad (3)$$

$$\text{LSI} = \sum \text{FR} \quad (4)$$

(LSI landslide susceptibility index; FR frequency ratios of each influencing factor)

The landslide susceptibility value represents the relative susceptibility to landslide occurrence. So the greater the frequency ratio value, the higher the susceptibility to landslide occurrence and the lower the value, the lower the susceptibility to landslide occurrence.

### Relative effect (RE) model

The relative effect model is based on the observed logarithmic relationships between distribution of landslides and each landslides-related factor. The main advantage of logarithmic function is in domain determination for output data which provides equal opportunity for plus and minus domains of calculated relative effect values (Ghafoori et al. 2006; Naveen Raj et al. 2011). Using the relative effect model (Eq. 5), the spatial relationships between landslide occurrence location and factors contributing to landslide occurrence were derived for each class in a landslide-influencing factor map.

$$\text{RE} = \text{Log} \left( \frac{\text{SR}}{\text{AR}} + \varepsilon \right) \quad (5)$$

$$\text{AR} = \frac{a}{A} \quad (6)$$

$$\text{SR} = \frac{\text{sld}}{\text{SLD}} \quad (7)$$

where RE is the relative effect,  $a$  is the total number of grids in individual class,  $A$  is the total number of grids in the study area, sld is the total number of landslide grids in the individual class, SLD is the total number of landslide grids in the study area and  $\varepsilon$  is a very small positive value near zero

$$\text{LSI} = \sum \text{RE} \quad (8)$$

In the present relationship analysis, there are following three cases for estimating relative effect of each class, based on its RE.

Negative effect—when the slide ratio is less than its class ratio, the RE value is less than zero. The case indicates that, it has an effect of decreasing landslide susceptibility.

Positive effect—when the slide ratio is greater than its class ratio, the RE value is greater than zero. The case indicates that, it has an effect of increasing landslide susceptibility.

Zero effect—when the slide ratio is equal to class ratio, the RE value is zero. This means that it has no effect of landslide susceptibility.

### Fuzzy set theory

Fuzzy set theory was first suggested by Zadeh (1965), which differs from the conventional Boolean set theory in such a manner objects within a set is definite. In the case of conventional set, the membership is 1 if the object is completely present in the set; if not in the set then the membership is 0. In fuzzy set, the extent of membership values of an object can have values ranges between 0 and 1, instead of having complete membership 0 or 1 as in a conventional set. The assignment of membership values between 0 and 1 is an important part in the fuzzy logic analysis. There is no regulation to assign the fuzzy membership values. The only thing is that the selected values must imitate the extent of membership of a set. It can be user defined based on subjective investigation (Bonham-Carter 1994) or the values can be derived from statistical analysis like information value (Yin and Yan 1988) and from frequency ratio (Lee 2007) or it can be assigned by various functions representing the reality such as J-shaped, sigmoidal and linear (Eastman 1995) or using analytical hierarchical method (Saaty 1978). With respect to a given data set (a thematic map), a membership can be assigned to each map category according to its direct/indirect relationship with the phenomena in consideration (Champati ray et al. 2007). The purpose of the integration of data is to combine various parameters collectively to explain and investigate relations to make conclusion about the problem under consideration. The method of integration of data may be based on complete statistical/quantitative approach, may be absolute knowledge based/qualitative method, where the lack or non-existence of sufficient data and may be the combination of both statistical as well as knowledge-driven method (Srivastava et al. 2010). A variety of operators can be employed to combine the membership values for the given two or more thematic maps with fuzzy membership functions for the same set. Bonham-Carter (1994)

discussed five operators, viz., the fuzzy AND, fuzzy OR, fuzzy algebraic product, fuzzy algebraic sum, and fuzzy gamma operator. This study uses the fuzzy gamma operator for combining the fuzzy membership values.

The fuzzy algebraic product is defined as:

$$\mu_{\text{combination}} = \prod_{i=1}^n \mu_i \tag{9}$$

The fuzzy algebraic sum is defined as:

$$\mu_{\text{combination}} = 1 - \prod_{i=1}^n (1 - \mu_i) \tag{10}$$

where,  $\mu_i$  is the fuzzy membership function for the ‘ $i$ ’ th map, and  $i = 1, 2, 3, \dots, n$  maps to be combined.

$$\mu_{\text{combination}} = (\text{FAS})^\gamma \times (\text{FAP})^{1-\gamma} \tag{11}$$

where,  $\gamma$  is a value chosen in the range 0–1; FAS-fuzzy algebraic sum; FAP-fuzzy algebraic product.

In the present study, the membership values for each thematic layer were derived by normalizing the probability frequency ratio values. However, the zero membership values have been assigned as 0.0001 to avoid the complete slackness of a class in a thematic map landslide hazard zonation analysis (Srivastava et al. 2010).

## Results and discussion

The frequency ratio (FR) and relative effect (RE) values were calculated using Eq. 1 and Eq. 5 and fuzzy membership values were normalized from frequency ratio values for all the classes present in entire parameter maps based on the relationship with past landslide locations (Table 1).

### Landslide susceptibility zonation

Landslide susceptibility analysis has been carried out through various methods. In the present study, the frequency ratio, fuzzy gamma operator, and relative effect models were adopted. For the application of frequency ratio, fuzzy gamma operator, and relative effect model, all the nine landslide causative factors were converted to a raster format with  $10 \times 10$  m size grids to calculate the landslide susceptibility index (LSI). The total number of study area grids was 18,645, and the total number of landslide grids in the study area was 54. All the influencing factors were taken to the spatial analysis extension of the ArcGIS software for integration. The LSI was calculated based on the integration rules as shown in Eqs. 4, 8, and 11. The integration was carried out using the raster calculator option of the ArcGIS software. If the LSI value is high, it means a higher susceptibility to landslide; a lower

**Table 1** Frequency ratio, relative effect and fuzzy membership values for landslide causative factors

Causative factors	Classes	No. of pixels in a class	% of pixels in a class	No. of landslide pixels in a class	% of landslide pixels in a class	FR	Fuzzy values	RE
Slope gradient	<13°	4,749	25.47	5	9.26	0.36	0.07	-0.44
	13°–22°	5,109	27.40	16	29.63	1.08	0.54	0.03
	22°–32°	4,877	26.16	19	35.19	1.35	0.71	0.13
	32°–45°	2,509	13.46	13	24.07	1.79	1.00	0.25
	45°–73°	1,401	7.51	1	1.85	0.25	0.00	-0.61
Slope aspect	Flat	752	4.03	1	1.85	0.46	0.32	-0.34
	North	1,088	5.84	2	3.70	0.63	0.43	-0.20
	Northeast	119	0.64	0	0.00	0.00	0.00	0.00
	East	503	2.70	1	1.85	0.69	0.48	-0.16
	Southeast	322	1.73	0	0.00	0.00	0.00	0.00
	South	164	0.88	0	0.00	0.00	0.00	0.00
	Southwest	1,693	9.08	1	1.85	0.20	0.14	-0.69
	West	6,867	36.83	19	35.19	0.96	0.66	-0.02
	Northwest	7,137	38.28	30	55.56	1.45	1.00	0.16
	Curvature	Concave (-)	6,917	37.10	12	22.22	0.60	0.00
Flat (0)		4,644	24.91	18	33.33	1.34	1.00	0.13
Convex (+)		7,084	37.99	24	44.44	1.17	0.77	0.07
Relief	280–426 m	5,488	29.43	3	5.56	0.19	0.00	-0.72
	426–618 m	3,012	16.15	10	18.52	1.15	0.37	0.06
	618–841 m	2,604	13.97	21	38.89	2.78	1.00	0.44
	841–1,040 m	3,131	16.79	17	31.48	1.87	0.65	0.27
	1,040–1,220 m	4,410	23.65	3	5.56	0.23	0.02	-0.63
Land use and land cover	Fairly dense forest	9,729	52.18	43	79.63	1.53	1.00	0.18
	Dense forest	7,260	38.94	10	18.52	0.48	0.31	-0.32
	Forest plantation	1,499	8.04	1	1.85	0.23	0.15	-0.64
	Settlement	157	0.84	0	0.00	0.00	0.00	0.00
Geology	Charnockite	10,639	57.06	41	75.93	1.33	1.00	0.12
	Hornblende-Biotite Gneiss	8,006	42.94	13	24.07	0.56	0.00	-0.25
Proximity to road	Road Buffer	1,967	10.55	54	100.00	9.48	1.00	0.98
	Other area	16,678	89.45	0	0.00	0.00	0.00	0.00
Proximity to drainage	0–64.03124237 m	4,427	23.74	3	5.56	0.23	0.00	-0.63
	64.03124238–130.3840485 m	5,068	27.18	11	20.37	0.75	0.34	-0.13
	130.3840486–194.1648712 m	4,328	23.21	22	40.74	1.76	1.00	0.24
	194.1648713–266.8332825 m	3,497	18.76	17	31.48	1.68	0.95	0.22
	266.8332826–388.3297424 m	1,325	7.11	1	1.85	0.26	0.02	-0.58
Proximity to lineaments	0–80.62257385 m	5,285	28.35	5	9.26	0.33	0.18	-0.49
	80.62257386–164.0121918 m	5,020	26.92	27	50.00	1.86	1.00	0.27
	164.0121919–252.3885956 m	4,175	22.39	19	35.19	1.57	0.84	0.20
	252.3885957–364.0054932 m	2,675	14.35	3	5.56	0.39	0.21	-0.41
	364.0054933–565.6854248 m	1,490	7.99	0	0.00	0.00	0.00	0.00

FR frequency ratio values, RE relative effect values, Fuzzy values fuzzy membership values

value means a lower susceptibility to landslides. For frequency ratio model, the minimum, mean, maximum and standard deviation of LSI are 2.590000153, 9.679908202,

23.31999969, and 3.924949664, respectively. For relative effect model, LSI values had a minimum value of -4.25, mean value of -0.614627511 and a maximum value of



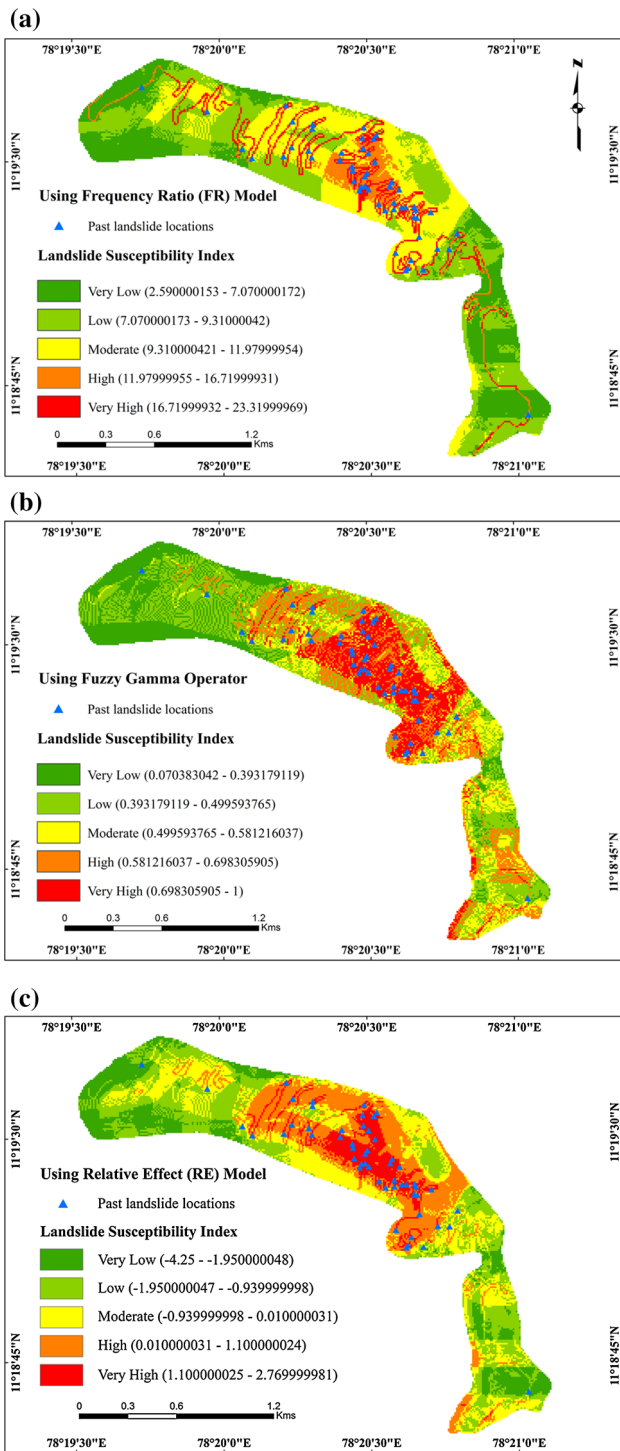


**Fig. 4** Landslide susceptibility maps. **a** Based on frequency ratio model, **b** based on fuzzy gamma operator (using  $\gamma = 0.975$ ), and **c** based on relative effect model

2.769999981, with a standard deviation of 1.258164037. In the case of fuzzy gamma operator, the value of  $\gamma$  was set to 0.1, 0.2, 0.3, 0.4, 0.5, 0.6, 0.7, 0.8, 0.9, 0.975, and 0.98 to observe its effect on the landslide susceptibility map. The

**Table 2** Percentage of known landslides falling into the different landslide susceptibility classes, determined by the frequency ratio, fuzzy gamma operator and relative effect models

Landslide susceptibility class	No. of pixels in class	% of class pixels	No. of landslides in class	% of landslide pixels in class
<b>Frequency ratio (FR) model</b>				
Very low	4,371	23.44	0	0.00
Low	6,371	34.17	1	1.85
Moderate	5,076	27.22	3	5.56
High	1,126	6.04	5	9.26
Very high	1,701	9.12	45	83.33
<b>Fuzzy gamma operator (FGO) model</b>				
Very low	3,537	18.97	0	0.00
Low	5,510	29.55	1	1.85
Moderate	2,914	15.63	1	1.85
High	3,629	19.46	11	20.37
Very high	3,055	16.39	41	75.93
<b>Relative effect (RE) model</b>				
Very low	2,786	14.94	0	0.00
Low	5,082	27.26	3	5.56
Moderate	4,908	26.32	2	3.70
High	4,181	22.42	11	20.37
Very high	1,688	9.05	38	74.07

integrated result with the gamma value ( $\gamma = 0.975$ ) was produced showing highest accuracy than other values tested in the present study. In the case of applying the gamma operator ( $\gamma = 0.975$ ), the minimum, mean, maximum, and standard deviation values of LSI are 0.070383042, 0.530481696, 1, and 0.150946113, respectively.

The landslide susceptibility maps (Fig. 4a, b, c) were classified into five susceptibility classes based on Jenks natural breaks classification method viz., very low, low, moderate, high and very high. The 54 known landslide locations were overlaid on the landslide susceptibility maps produced by frequency ratio, relative effect, and fuzzy gamma operator models, and the percentage of pixels of known landslides under various susceptibility classes was calculated. The frequency ratio model identified 92.59 % of the known landslides were concentrated in the high and very high susceptibility classes, whereas relative effect model predicted 94.44 % of the known landslides in the high and very high susceptibility classes. The fuzzy gamma operator model ( $\gamma = 0.975$ ) possesses 96.30 % of the known landslides in the high and very high susceptibility classes. The percentage of landslide occurrence in each susceptibility class for all the three models is shown in Table 2 and as a bar diagram in Fig. 5.

**Fig. 5** Relationship between landslide frequencies with susceptibility classes

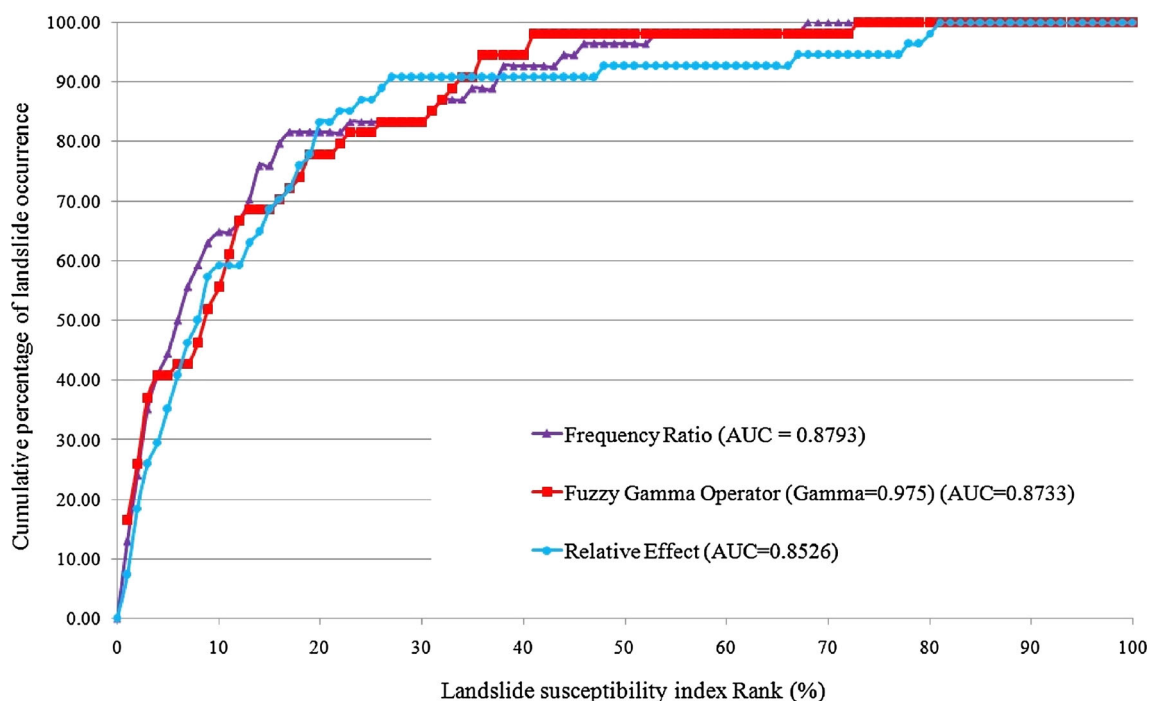
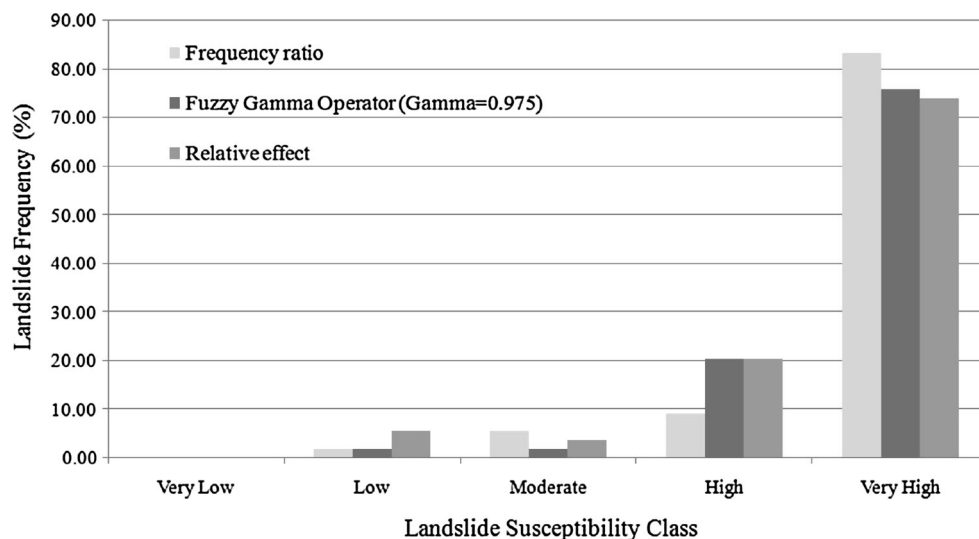


**Fig. 6** Illustration of success rate curve showing landslide susceptibility index rank ( $x$ -axis) occurring in cumulative percent of landslide occurrence ( $y$ -axis)

### Comparison and validation of the models

The Area Under Curve (AUC) is one of the most commonly used qualitative accuracy assessment method for the prediction models in natural hazard assessment (Beguieria 2006; Pradhan and Lee 2009). The success rate describes how well the model and factor predict the landslide (Chung and Fabbri 1999). The accuracy of frequency ratio, fuzzy gamma operator, relative effect models in landslide susceptibility mapping in the Kolli hills was evaluated by

calculating “area under the curve (AUC)”. The validation of landslide susceptibility analysis result was achieved by comparing the known landslide location data with the landslide susceptibility maps. The success rate curves were produced and the “area under the curve (AUC)” was calculated for all the three susceptibility maps using the existing landslide location data. To obtain a relative landslide susceptibility index ranks for each prediction model, the calculated index values of all grids in the study area were sorted in descending order. Then the ordered cell

values were divided into 100 classes, with accumulated 1 % intervals. An ideal model shows an AUC value close to 1.0, whereas a value close to 0.5 indicates inaccuracy in the model (Fawcett 2006). The AUC value of success rate curve for relative effect model was found to be 0.8526. The AUC value for landslide susceptibility map produced by fuzzy gamma operator (using  $\gamma = 0.975$ ) was calculated as 0.8733. The AUC value for frequency ratio model showed highest accuracy of 0.8793. The comparison result of success rate curve is shown as a line graph in Fig. 6. These results point out that frequency ratio model shows good prediction pattern than fuzzy gamma operator and relative effect model of landslide susceptibility in the study area. Moreover, the success rate curve for frequency ratio model had a greater steepness in the first part of the curve, signifying its greater predictive capability (Nandi and Shakoor 2009).

**Conclusions**

In the present study, frequency ratio, fuzzy gamma operator, and relative effect models were adopted for the landslide susceptibility mapping along Ghat road section of Kolli hills, Tamil Nadu. Landslide susceptibility maps have been produced using the relationship between each landslide-influencing parameters and known landslide locations. The results have shown that the occurrence of landslides were more prominent along cut slope, slope gradient in 32°–45°, convex curvature, and relief in 618–1,040 m categories. The validation results show that the frequency ratio model has better prediction accuracy (AUC = 0.8793) than the fuzzy gamma operator model (AUC = 0.8733) and relative effect model (AUC = 0.8526). The landslide susceptibility maps are the source for decision making and developmental activities in an area. Hence, the output results of the present study can help the developers, planners, and engineers for slope management and land-use planning in the study area.

**Acknowledgments** The authors acknowledge the Natural Resources Data Management System (NRDMS), Department of Science and Technology, New Delhi, for supporting the project. The authors also thank State Highways and Horticulture departments for providing landslide event and rainfall data.

**References**

AGS (2007) Guidelines for landslide susceptibility, hazard and risk zoning for land use planning. *Aust Geomech* 42:13–36  
 Ahmad M, Ansari MK, Singh TN (2013) Instability investigations of basaltic soil slopes along SH-72. *Geomatics, Natural Hazards and Risk*, Nashik. doi:10.1080/19475705.2013.826740

Akgul A, Bulut F (2007) GIS-based landslide susceptibility for Arsin-Yomra (Trabzon, North Turkey) region. *Environ Geol* 51(8):1377–1387  
 Akgun A, Dag S, Bulut F (2008) Landslide susceptibility mapping for a landslide-prone area (Findikli, NE of Turkey) by likelihood-frequency ratio and weighted linear combination models. *Environ Geol* 54(6):1127–1143  
 Aleotti P, Chowdhury R (1999) Landslide hazard assessment: summary review and new perspectives. *Bull Eng Geol Environ* 58:21–44  
 Anbalagan R (1992) Landslide hazard evaluation and zonation mapping in mountainous Terrain. *Eng Geol* 32:269–277  
 Anbazhagan S, Ramesh V (2014) Landslide hazard zonation mapping in Ghat road section of Kolli hills, India. *J Mt Sci* 11(5):1308–1325  
 Anbazhagan S, Neelakantan R, Arivazhagan S, Vanaraju G (2008) Developments of fractures and land subsidence at Kolli hills, Tamil Nadu. *J Geol Soc India* 72:348–352  
 Anderson MG, Holcombe E (2013) Community-based landslide risk reduction-managing disasters in small steps. Library of Congress Cataloging-in-Publication Data. The World Bank, Washington, DC  
 Atkinson PM, Massari R (1998) Generalized linear modeling of susceptibility to landsliding in the central Apennines, Italy. *Comput Geosci* 24:373–385  
 Ayalew L, Yamagishi H, Ugawa N (2004) Landslide susceptibility mapping using GIS based weighted linear combination, the case in Tsugawa area of Agano River, Niigata Prefecture, Japan. *Landslides* 1:73–81  
 Begueria S (2006) Validation and evaluation of predictive models in hazard assessment and risk management. *Nat Hazards* 37:315–329  
 Bonham-Carter GF (1994) Geographic information systems for geoscientists: modelling with GIS. Elsevier Butterworth-Heinemann, Oxford, pp 292–302  
 Brabb EE (1984) Innovative approaches to landslide hazard and risk mapping. Proceedings of 4th International Symposium on Landslides, Totonto, Canada, vol 1. BiTech Publishers, Vancouver, pp 307–324  
 Caniani D, Pascale S, Sdao F, Sole A (2008) Neural networks and landslide susceptibility: a case study of the urban area of Potenza. *Nat Hazards* 45(1):55–72  
 Capecchi F, Focardi P (1988) Rainfall and landslides: research into a critical precipitation coefficient in an area of Italy. In: Bonnard C (ed) Proceedings of the 5th International Symposium on Landslides. A.A. Balkema, Lausanne, Rotterdam, pp 1031–1136  
 Carrara A, Cardinali M, Detti R, Guzzetti F, Pasqui V, Reichenbach P (1991) GIS technique and statistical models in evaluating landslide hazard. *Earth Surf Process Land Forms* 16:427–445  
 Catani F, Lagomarsino S, Segoni S, Tofani V (2013) Landslide susceptibility estimation by random forests technique: sensitivity and scaling issues. *Nat Hazards Earth Syst Sci* 13:2815–2831  
 Champati Ray PK, Dimri S, Lakhera RC, Sati S (2007) Fuzzy-based method for landslide hazard assessment in active seismic zone of Himalaya. *Landslides* 4:101–111  
 Chauhan S, Sharma M, Arora MK, Gupta NK (2010) Landslide susceptibility zonation through ratings derived from artificial neural network. *Int J Appl Earth Obs Geoinf* 12:340–350  
 Choi J, Oh HJ, Lee HJ, Lee C, Lee S (2012) Combining landslide susceptibility maps obtained from frequency ratio, logistic regression, and artificial neural network models using ASTER images and GIS. *Eng Geol* 124:12–23  
 Chung C-JF, Fabbri AG (1999) Probabilistic prediction models for landslide hazard mapping. *Photogramm Eng Remote Sens* 65(12):1389–1399

- Corominas J, Moya J (2008) A review of assessing landslide frequency for hazard zoning purposes. *Eng Geol* 102:193–213
- Dai FC, Lee CF (2002) Landslide characteristics and slope instability modeling using GIS: Lantau Island, Hong Kong. *Geomorphology* 42:213–228
- Dai FC, Lee CF, Li J, Xu ZW (2001) Assessment of landslide susceptibility on the natural terrain of Lantau Island, Hong Kong. *Environ Geol* 40:381–391
- Dai FC, Lee CF, Ngai YY (2002) Landslide risk assessment and management: an overview. *Eng Geol* 64(1):65–87
- Das I, Sahoo S, van Weston C, Stein A, Hack R (2010) Landslide susceptibility assessment using logistic regression and its comparison with a rock mass classification system, along a road section in the northern Himalayas (India). *Geomorphology* 114:627–637
- Das I, Stein A, Kerle N, Dadhwal VK (2011) Probabilistic landslide hazard assessment using homogeneous susceptible units (HSU) along a national highway corridor in the northern Himalayas, India. *Landslides* 8:293–308
- Devoli G, Morales A, Hoeg K (2007) Historical landslides in Nicaragua—collection and analysis of data. *Landslides* 4(1):5–18
- Duman TY, Can T, Gokceoglu C, Nefeslioglu HA, Sonmez H (2006) Application of logistic regression for landslide susceptibility zoning of Cekmece Area, Istanbul, Turkey. *Environ Geol* 51(2):241–256
- Eastman JR (1995) Decision Support. In: Idrisi for Windows: user's guide version 1.0. Clark Labs for Cartographic Technology and Geographic Analysis. Clark University, Worcester, Massachusetts
- Ehret D, Rohn J, Dumperth C, Eckstein S, Ernstberger S, Otte K, Rudolph R, Wiedenmann J (2010) Frequency ratio analysis of mass movements in the Xiangxi catchment, three Gorges reservoir area, China. *J Earth Sci* 21(6):824–834
- Ercanoglu M, Gokceoglu C (2001) Assessment of landslide susceptibility for a landslide-prone area (north of Yenice, NW Turkey) by fuzzy approach. *Environ Geol* 41:720–730
- Ercanoglu M, Gokceoglu C (2004) Use of fuzzy relations to produce landslide susceptibility map of a landslide prone area (West Black Sea Region, Turkey). *Eng Geol* 75:229–250
- Fawcett T (2006) An introduction to ROC analysis. *Pattern Recogn Lett* 27:861–874
- Fernandez Merodo JA, Pastor M, Mira P (2004) Modeling of diffuse failure mechanisms of catastrophic landslides. *Comput Methods Appl Mech Eng* 193:2911–2939
- Ghafoori M, Sadeghi H, Lashkaripour GR, Alimohammadi B (2006) Landslide hazard zonation using relative effect method. The Geological Society of London, IAEG Paper number 474
- GSI (1995) Geological and mineral map of Tamil Nadu and Pondicherry. Published in 1:500,000 scale by the Director General, Geological Survey of India
- GSI Report (2006) Geology and mineral resources of the states of India. Part IV-Tamil Nadu and Pondicherry
- Gupta RP, Joshi BC (1990) Landslide hazard zoning using the GIS approach—a case study from the Ramganga catchment, Himalayas. *Eng Geol* 28:119–131
- Guzzetti F, Carrara A, Cardinali M, Reichenbach P (1999) Landslide hazard evaluation: a review of current techniques and their application in a multi-case study, central Italy. *Geomorphology* 31:181–216
- Jenks GF (1967) The data model concept in statistical mapping. *Int Year Book Cartogr* 7:186–190
- Kannan M, Saranathan E, Anbalagan R (2013) Landslide vulnerability mapping using frequency ratio model: a geospatial approach in Bodi-Bodimettu Ghat section, Theni district, Tamil Nadu, India. *Arab J Geosci* 6(8):2901–2913
- Kanungo DP, Arora MK, Sarkar S, Gupta RP (2006) A comparative study of conventional, ANN black box, fuzzy and combined neural and fuzzy weighting procedures for landslide susceptibility zonation in Darjeeling Himalayas. *Eng Geol* 85:347–366
- Kanungo DP, Arora MK, Sarkar S, Gupta RP (2009) A fuzzy set based approach for integration of thematic maps for landslide susceptibility zonation. *Georisk* 3(1):30–43
- Kavitha M, Petrou M, Tarantino C, Blonda P (2008) Landslide possibility mapping using fuzzy approaches. *IEEE Trans Geosci Remote Sens* 46(4):1253–1265
- Kienholz H, Schneider G, Bichsel M, Grunder M, Mool P (1984) Mapping of mountain hazards and slope stability. *Mt Res Dev* 4(3):247–266
- Lee S (2005) Application of logistic regression model and its validation for landslide susceptibility mapping using GIS and remote sensing data. *Int J Remote Sens* 26:1477–1491
- Lee S (2007) Application and verification of fuzzy algebraic operators to landslide susceptibility mapping. *Environ Geol* 52:615–623
- Lee S, Pradhan B (2006) Probabilistic landslide hazards and risk mapping on Penang Island, Malaysia. *J Earth Syst Sci* 115(6):661–672
- Lee S, Pradhan B (2007) Landslide hazard mapping at Selangor, Malaysia using frequency ratio and logistic regression models. *Landslides* 4:33–41
- Lee S, Talib JA (2005) Probabilistic landslide susceptibility and factor effect analysis. *Environ Geol* 47:982–990
- Lee S, Choi J, Min K (2002) Landslide susceptibility analysis and verification using the Bayesian probability model. *Environ Geol* 43:120–131
- Lee S, Ryu JH, Min K, Won JS (2003) Landslide susceptibility analysis using GIS and artificial neural network. *Earth Surf Proc Land* 27:1361–1376
- Lee S, Choi J, Woo I (2004) The effect of spatial resolution on the accuracy of landslide susceptibility mapping: a case study in Boun, Korea. *Geosci J* 8(1):51–60
- Lee S, Ryu JH, Lee MJ, Won JS (2006) The application of artificial neural networks to landslide susceptibility mapping at Janghung, Korea. *Math Geol* 38:199–220
- Mantovani F, Soeters R, Van Westen CJ (1996) Remote sensing techniques for landslide studies and hazard zonation in Europe. *Geomorphology* 15:213–225
- Mark RK, Ellen SD (1995) Statistical and simulation models for mapping debris-flow hazard, geographical information systems in assessing natural hazards. In: Carrara A, Guzzetti F (ed.) Kluwer Academic Publishers, Dordrecht. pp 93–106
- McKean J, Buechel S, Gaydos L (1991) Remote sensing and landslide hazard assessment. *Photogramm Eng Remote Sens* 57(9):1185–1193
- Mostyn GR, Fell R (1997) Quantitative and semiquantitative estimation of the probability of landslides in landslide risk assessment. In: Cruden D, Fell R (eds) Balkema, Balkema, Rotterdam, pp 297–315
- Nandi A, Shakoor A (2008) Application of logistic regression model for slope instability prediction in Cuyahoga river watershed, Ohio, USA. *Georisk* 2(1):16–27
- Nandi A, Shakoor A (2009) A GIS-based landslide susceptibility evaluation using bivariate and multivariate statistical analyses. *Eng Geol* 110:11–20
- Naranjo JL, van Westen CJ, Soeters R (1994) Evaluating the use of training areas in bivariate statistical landslide hazard analysis—a case study in Columbia. *ITC J* 3:292–300
- Naveen Raj T, Ram mohan V, Backiaraj S, Muthusamy S (2011) Landslide hazard zonation using the relative effect method in south eastern part of Nilgiris, Tamil Nadu, India. *Int J Eng Sci Technol* 3(4):3260–3266

- Ohlmacher GC, Davis JC (2003) Using multiple logistic regression and GIS technology to predict landslide hazard in northeast Kansa, USA. *Eng Geol* 69:331–343
- Okimura T (1982) Situation of surficial slope failure based on the distribution of soil layer. *Shin-sabo* 35:9–18 (in Japanese with English abstract)
- Okimura T, Kawatani T (1986) Mapping of the potential surface-failure sites on granite mountain slopes. In: Gardiner V (ed) *International geomorphology, Part I*. Wiley, New York, pp 121–138
- Pachauri AK, Pant M (1992) Landslide hazard mapping based on geological attributes. *Eng Geol* 32:81–100
- Poudyal CP, Chang C, Oh HJ, Lee S (2010) Landslide susceptibility maps comparing frequency ratio and artificial neural networks: a case study from the Nepal Himalaya. *Environ Earth Sci* 61:1049–1064
- Pradhan B, Lee S (2007) Utilization of optical remote sensing data and GIS tools for regional landslide hazard analysis using an artificial neural network model. *Earth Sci Front* 14(6):143–152
- Pradhan B, Lee S (2009) Delineation of landslide hazard areas on Penang Island, Malaysia, by using frequency ratio, logistic regression, and artificial neural network models. *Environ Earth Sci* 60:1037–1054
- Pradhan B, Lee S (2010a) Regional landslide susceptibility analysis using back-propagation neural network model at Cameron Highland, Malaysia. *Landslides* 7:13–30
- Pradhan B, Lee S (2010b) Landslide susceptibility assessment and factor effect analysis: backpropagation artificial neural networks and their comparison with frequency ratio and bivariate logistic regression modelling. *Environ Model Softw* 25:747–759
- Pradhan B, Lee S, Mansor S, Buchroithner M, Jamaluddin N, Khujaimah Z (2008) Utilization of optical remote sensing data and geographic information system tools for regional landslide hazard analysis by using binomial logistic regression model. *J Appl Remote Sens* 2(1):1–11
- Pradhan B, Lee S, Buchroithner MF (2009) Use of geospatial data and fuzzy algebraic operators to landslide-hazard mapping. *Appl Geomat* 1:3–15
- Ramani SE, Pitchaimani K, Gnanamanickam VR (2011) GIS based landslide susceptibility mapping of TevankaraiAr sub-watershed, Kodaikkanal, India using binary logistic regression analysis. *J Mt Sci* 8(4):505–517
- Saaty TL (1978) Exploring the interface between hierarchies, multiple objectives and fuzzy set. *Fuzzy Sets Syst* 1:57–68
- Sarkar S, Kanungo DP (2004) An integrated approach for landslide susceptibility mapping using remote sensing and GIS. *Photogramm Eng Remote Sens* 70(5):617–625
- Sarkar S, Kanungo DP, Mehrotra GS (1995) Landslide hazard zonation: a case study in Garhwal Himalaya, India. *Mt Res Dev* 15(4):301–309
- Singh PK, Kainthola A, Singh TN (2013a) Rock mass assessment along the right bank of river Sutlej, Luhri, Himachal Pradesh, India. *Geomat Nat Hazards Risk Online*. doi:10.1080/19475705.2013.834486
- Singh R, Umrao RK, Singh TN (2013b) Stability evaluation of road-cut slopes in the Lesser Himalaya of Uttarakhand, India: conventional and numerical approaches. *Bull Eng Geol Environ*. doi:10.1007/s10064-013-0532-1
- Skempton AW, Delory EA (1957) Stability of natural slopes in London clay. In: *Proceedings of 4th International Conference on Soil Mechanics and Foundation Engineering*, vol 2. Butterworths, London, pp 378–381
- Srivastava V, Srivastava H, Lakhera RC (2010) Fuzzy gamma based geomatic modeling for landslide hazard susceptibility in a part of Tons river valley, northwest Himalaya, India. *Geomat Nat Hazards Risk* 1(3):225–242
- Sujatha ER, Rajamanickam GV, Kumaravel P (2012) Landslide susceptibility analysis using probabilistic certainty factor approach: a case study on Tevankarai stream watershed, India. *J Earth Syst Sci* 121(5):1337–1350
- Tunusluoglu MC, Gokceoglu C, Nefeslioglu HA, Sonmez H (2008) Extraction of potential debris source areas by logistic regression technique: a case study from Barla, Besparmak and Kapi mountains (NW Taurids, Turkey). *Environ Geol* 54(1):9–22
- Varnes DJ (1984) Landslide hazard zonation: a review of principles and practice. *International association of engineering geology*, vol 3. UNESCO, Paris
- Wang HB, Sassa K (2005) Comparative evaluation of landslide susceptibility in Minamata area, Japan. *Environ Geol* 47:956–966
- Wang SQ, Unwin DJ (1992) Modeling landslide distribution on loess soils in China: an investigation. *Int J Geogr Inf Syst* 6:391–405
- Wieczorek GF (1984) Preparing a detailed landslide-inventory map for hazard evaluation and reduction. *Bull Assoc Eng Geol* 21:337–342
- Yilmaz I (2009a) Landslide susceptibility mapping using frequency ratio, logistic regression, artificial neural networks and their comparison: a case study from Kat landslides (Tokat-Turkey). *Comput Geosci* 35:1125–1138
- Yilmaz I (2009b) A case study from Koyulhisar (Sivas-Turkey) for landslide susceptibility mapping by artificial neural networks. *Bull Eng Geol Environ* 68:297–306
- Yilmaz I, Keskin I (2009) GIS based statistical and physical approaches to landslide susceptibility mapping (Sebinkarahisar, Turkey). *Bull Eng Geol Environ* 68:459–471
- Yilmaz I, Marschalko M, Bednarik M (2012) Comments on “Landslide susceptibility zonation study using remote sensing and GIS technology in the Ken-Betwa River Link area, India” by Avtar R, Singh CK, Singh G, Verma RL, Mukherjee S, Sawada H, in *Bulletin of Engineering Geology and the Environment* (doi:10.1007/s10064-011-0368-5). *Bull Eng Geol Environ* 71(4):803–805. doi:10.1007/s10064-011-0406-3
- Yin KL, Yan TZ (1988) Statistical prediction model for slope instability of metamorphosed rocks. In: *Proceedings of the 5th international symposium on landslides*, vol 2. A.A. Balkema, Lausanne, Rotterdam, pp 1269–1272
- Zadeh LA (1965) Fuzzy sets. *IEEE Inf Control* 8:125–151